

Multiple regimes of diffusion

B. Mehlig,¹ M. Wilkinson,² V. Bezuglyy,² K. Gustavsson,¹ and K. Nakamura³

¹*Department of Physics, Gothenburg University, 41296 Gothenburg, Sweden*

²*Department of Mathematics and Statistics, The Open University, Walton Hall, Milton Keynes MK7 6AA, United Kingdom*

³*Department of Applied Physics, Osaka City University, Osaka 558-8585, Japan and Department of Heat Physics, Uzbek Academy of Sciences, 28 Katartal Street, 100135 Tashkent, Uzbekistan*

(Received 21 January 2009; revised manuscript received 20 April 2009; published 28 July 2009)

We consider the diffusion of independent particles experiencing random accelerations by a space- and time-dependent force as well as viscous damping. This model can exhibit several asymptotic behaviors, depending upon the limiting cases which are considered, some of which have been discussed in earlier work. Here, we explore the full space of dimensionless parameters and present an “asymptotic phase diagram” which delineates the limiting regimes.

DOI: [10.1103/PhysRevE.80.011139](https://doi.org/10.1103/PhysRevE.80.011139)

PACS number(s): 05.40.-a, 05.45.-a, 05.60.Cd

I. INTRODUCTION

The position x of a particle subjected to a force which fluctuates randomly in time t might be expected to undergo diffusion in the sense that

$$\lim_{t \rightarrow \infty} \frac{\langle x^2(t) \rangle}{2t} = \mathcal{D}_x \quad (1)$$

for some diffusion coefficient \mathcal{D}_x , provided that there is some damping mechanism preventing the particle from being accelerated to arbitrarily high velocities [in Eq. (1), angular brackets denote averages over realizations of the random force].

In this paper, we determine the diffusion constant for the simplest model for this process in one spatial dimension, in which the equation of motion of the particle is

$$m\dot{x} = p, \quad \dot{p} = -\gamma p + f(x, t). \quad (2)$$

Here x and p are particle position and momentum, respectively, m is the mass, and γ is the rate at which the particle momentum is damped due to viscous drag. Time derivatives are denoted by dots. Further, the random forcing $f(x, t)$ is modeled by a Gaussian random function with zero mean and with correlation function $C(x, t)$, characterized by a correlation length ξ , correlation time τ , and of typical size σ

$$\langle f(x, t) \rangle = 0, \quad \langle f(x, t) f(x', t') \rangle = C(x - x', t - t') \quad (3)$$

The dynamics of the model defined by Eqs. (2) and (3) is determined by five dimensional parameters: σ , τ , ξ , the mass m , and γ . Out of these, one can form two independent dimensionless parameters: a dimensionless force $\chi = \sigma\tau^2 / (m\xi)$ and a dimensionless damping $\omega = \gamma\tau$. In the following, we explore the full space of dimensionless parameters χ and ω .

There is no exact expression for the diffusion constant for this simple model. However, asymptotic expressions with different regions of validity are known, depending on which ratios of dimensionless parameters, ω and χ , approach zero. We show that there are surprisingly many different asymptotic regimes, which are summarized in an “asymptotic phase diagram” (Fig. 1). The axes in this diagram are logarithms of two independent dimensionless parameters of the model, and a ray from the origin with slope μ

represents a limiting process where χ approaches 0 or ∞ with $\omega \sim \chi^\nu$. The phase lines do not indicate sharp transitions, but rather the boundaries between the domains of validity of six different asymptotic regimes as the limit is taken. Some of the regimes are well understood, but others are either new or have only been studied recently by the authors of this paper. It is remarkable that the phase diagram of such a fundamental model for diffusion processes has not been completely characterized before now. In all cases, the long-time dynamics is diffusive, but in some of the regimes, the stationary distribution of momentum may be strongly non-Gaussian and the short-time behavior may exhibit anomalous diffusion that is $\langle x^2(t) \rangle \propto t^\nu$ with $\nu \neq 1$. The diffusion constant \mathcal{D}_x depends in different ways on the microscopic parameters in different regimes, as illustrated in Fig. 2.

The three-dimensional version of the model defined by Eqs. (2) and (3) arises naturally in the study of small particles suspended in a randomly moving fluid, for which motion relative to the fluid is determined by viscous drag. In

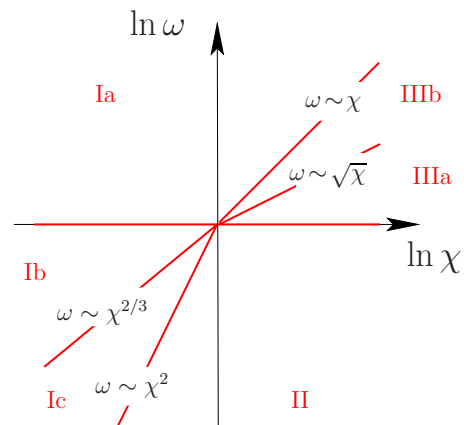


FIG. 1. (Color online) Asymptotic phase diagram (schematic) for the model defined by Eqs. (2)–(4) summarizing the different dynamical behaviors of Eq. (2) described in Secs. III–V: I Ornstein-Uhlenbeck, II generalized Ornstein-Uhlenbeck, IIIb overdamped minimum tracking, and IIIa underdamped minimum tracking. The Ornstein-Uhlenbeck regime is divided into three regions: overdamped advection (Ia), underdamped advection (Ib), and underdamped inertial dynamics (Ic).

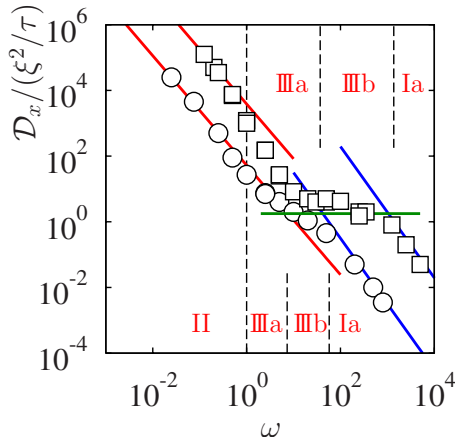


FIG. 2. (Color online) Illustration of multiple regimes of diffusion. Evaluation of the diffusion constant \mathcal{D}_x for constant χ as a function of ω : for $\chi=50$ (circles) and $\chi=1250$ (squares). Also shown is the expected behavior in regime I [Eq. (15)] (blue solid lines) and the expected behavior in regime II [Eq. (31)] (red solid lines). Finally, the estimate Eq. (42) for \mathcal{D}_x in the minimum-tracking regime is shown (green horizontal line).

that context, the random force is replaced by a random vector field, which would usually be chosen to be solenoidal, to represent an incompressible flow. This three-dimensional system has been extensively studied in certain limits. A significant early contribution is due to Maxey [1], who analyzed the clustering of particles suspended in a turbulent fluid (referred to as preferential concentration). Reference [2] provides an overview of the literature on this problem and describes recent progress.

This present paper explores the full range of regimes which are possible in limiting cases of the model, some of which are not realized in fluid-dynamical applications. We remark that different choices of dimensionless parameters are used in some other papers: much of the fluid-dynamics literature use the Stokes number $St=1/\omega$ as a measure of the damping and the Kubo number $Ku=\chi/\omega$ as a measure of the time scale of fluctuations of the velocity field.

The model also exhibits an interesting effect which involves a phase transition in the conventional sense. Depending on the dimensionless parameters of the model, particles with different initial conditions experiencing the same realization of the random force approach the same trajectory with probability unity. This “path-coalescence” effect and the “path-coalescence transition” where it disappears were noted by Deutsch [3], who appears to have been the first to consider this model systematically. In this paper, we also describe the full phase line for the path-coalescence transition, extending results of [4]. The critical line for the path-coalescence transition in the χ - ω plane is shown in Fig. 3.

The numerical simulations of Eqs. (2) and (3) described in this paper were performed with the following choice of correlation function:

$$C(x, t) = \sigma^2 \exp[-x^2/(2\xi^2) - t^2/(2\tau^2)], \quad (4)$$

describing a random force with locally smooth spatial and time correlations. Apart from this requirement, the precise

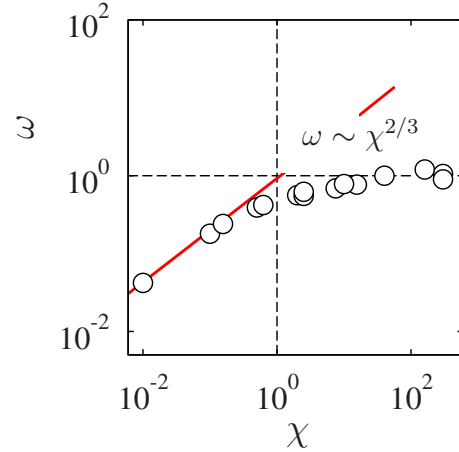


FIG. 3. (Color online) Phase line of the path-coalescence transition. Results of computer simulations of Eqs. (2)–(4) for the phase line of the path-coalescence transition. Also shown is the theoretical result valid for small values of χ (red solid line).

functional form of the correlation function is not significant. Note however that in regime II, one aspect of the random forcing can make a qualitative difference (see Sec. VI). For any choice of the random force, there is a corresponding potential, satisfying $-\partial V(x, t)/\partial x = f(x, t)$. For a generic choice of correlation function, the one-dimensional potential $V(x, t)$ corresponding to the force $f(x, t)$ performs a random walk exhibiting increasing fluctuations as $|x|$ increases. We also consider cases where the particle dynamics is different if the potential $V(x, t)$ is a stationary random process.

The different regimes are illustrated in Fig. 4 by numerical simulations of Eqs. (2)–(4). This figure shows the trajectories $x(t)$ of several particles for a given realization $f(x, t)$ of the forcing.

II. SUMMARY AND PHYSICAL DESCRIPTION OF THE REGIMES

Before describing our results in detail, we discuss the physics of the parameter regimes of our model. We also mention connections with other work on the dynamics of randomly forced particles, where some of the regimes of our model have been studied.

In the limit of large damping, the particles are advected by a random velocity field: there is extensive literature on this problem and the closely related model of passive scalars [5]. The advective case corresponds to regime Ia in our model.

Our model [Eqs. (2) and (3)] reduces to the well-known Ornstein-Uhlenbeck process [6] when the position dependence of the force can be neglected. This is the case when the forcing is sufficiently weak so that the particle position changes negligibly within correlation time τ , which is the case of weak forcing and weak damping. This condition will be made more precise below. The Ornstein-Uhlenbeck process is discussed in standard textbooks (see, for example, [7]). The regimes Ib and Ic can both be analyzed by treating the evolution of the momentum as an Ornstein-Uhlenbeck process. The difference between these two regimes is that

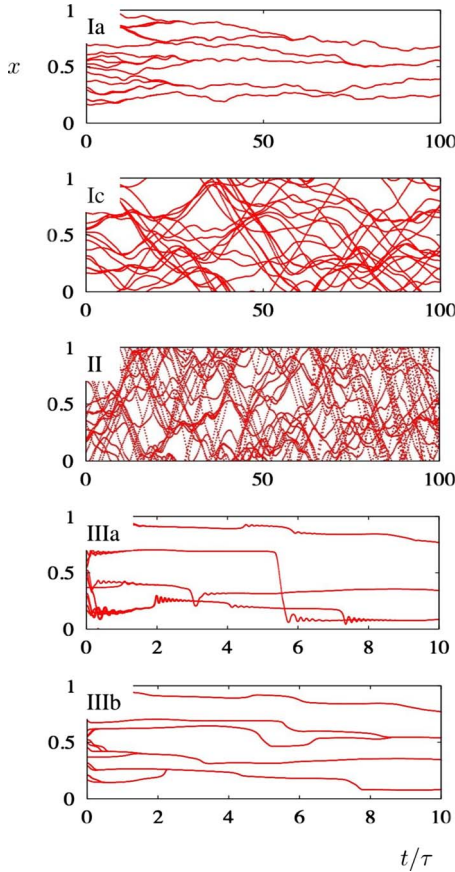


FIG. 4. (Color online) Trajectories $x(t)$ as a function of t/τ for 20 particles with initial condition $p(0)=0$ and $x(0)$ randomly chosen in $[0,1]$. The first two pictures (in regimes Ia and Ic) are similar to those obtained by Deutsch [3] and to Fig. 1 in Ref. [4]. The trajectories in region Ib are similar to those in Ia (not shown). The difference between regimes IIIa and IIIb is that there are oscillations in regime IIIa due to smaller damping.

regime Ib exhibits path coalescence whereas regime Ic does not. Despite the fact that regime Ia describes an overdamped process, the formula for the diffusion constant is the same as for the Ornstein-Uhlenbeck process. For this reason, regimes Ia, Ib, and Ic are treated together in Sec. III and are referred to as the Ornstein-Uhlenbeck regimes.

Our model is also related to stochastic or “Fermi” acceleration of classical particles by random forces, which is used to model the production of cosmic rays [8]. In these studies the damping term (proportional to γ) is not included in the equation of motion and the particle is accelerated to arbitrarily high energies. The treatment of the random forcing term in the case where the particle is rapidly moving, first considered in [9], is used in our description of regime II. Without damping, the model exhibits anomalous diffusion [10,11]. For the case where the damping term is included, a new dynamical regime was identified in [12,13] with a non-Maxwellian velocity distribution (as well as anomalous diffusion at short times, before the damping term starts to limit the acceleration). This is regime II in the phase diagram Fig. 1, we call it the “generalized Ornstein-Uhlenbeck regime.” It is discussed in Sec. IV.

In the case where both the damping and the force are strong, the particle follows a local minimum of the potential $V(x,t)$. This is regime III of the phase diagram. This “minimum-tracking” regime has not been considered in detail in earlier work. It is discussed in Sec. V below. In Sec. VI we briefly describe how results for regime II differ for more general types of forcing, such as the case where $V(x,t)$ has stationary statistics.

Figure 3 shows numerical results on the path-coalescence transition, for the choice of correlation function Eq. (4). For small values of χ , the phase boundary is in precise agreement with an asymptotic theory discussed in [4], which shows that the transition line is determined by the condition $\omega\chi^{-2/3} \rightarrow \text{const.}$ in the limit as $\chi \rightarrow 0$. The data for large χ are consistent with the hypothesis that the phase line approaches $\omega = \text{const.}$ as $\chi \rightarrow \infty$, but we have no compelling argument to support this.

Finally, we comment on the physically accessible range of dimensionless parameters. This depends on the nature of the forcing. In the case of a particle suspended in a turbulent fluid flow with velocity field $u(x,t)$, the random forcing is due to viscous drag and we write $f(x,t) = m\gamma u(x,t)$. In this case, disturbances in the fluid velocity field $u(x,t)$ are transported by $u(x,t)$ itself. This implies that the Kubo number $\text{Ku} \equiv u\tau/\xi$ cannot be large (equivalently, χ cannot be large compared to ω) if the random forcing is due to a fluid flow. In other cases, such as forcing by random electromagnetic fields, the entire phase diagram may be accessible.

III. ORNSTEIN-UHLENBECK REGIME

We term the regimes Ia, Ib, and Ic in the phase diagram Fig. 1 the “Ornstein-Uhlenbeck regimes.” In these regimes, the particles move so slowly that the distance traveled during one correlation time τ of the random force $f(x,t)$ is much smaller than its correlation length ξ . Thus changes in the spatial argument do not contribute significantly to the decorrelation of $f(x,t)$ and one may approximate $f[x(t),t] \approx f[x(0),t]$ for times t of the order of or less than the correlation time τ .

Regime I is divided into one overdamped regime, regime Ia ($\omega \gg 1$), and two underdamped regimes, Ib and Ic ($\omega \ll 1$).

In the overdamped regime Ia, the acceleration term in Eq. (2) is negligible and consequently the particles are advected by the random force, that is, $\dot{x} \approx f(x,t)/(m\gamma)$.

The two regimes Ib and Ic are distinguished by different behaviors of nearby particles, as can be seen in Fig. 4. In regime Ib, initially separate but nearby particle trajectories approach each other (path-coalescence regime). In regime Ic, by contrast, initially close particle trajectories do not coalesce. In the remainder of this section, we first briefly describe the single-particle dynamics in this regime (diffusion) and then summarize what is known about the path-coalescence transition.

To describe diffusion in the overdamped regime, one integrates the advective equation of motion $\dot{x} = f(x,t)/(m\gamma)$. The change in position δx during a short-time interval $\delta t \gg \tau$ is

$$\delta x = \frac{1}{m\gamma} \int_t^{t+\delta t} dt_1 f[x(t_1), t_1]. \quad (5)$$

We note that the time dependence of $f[x(t), t]$ is smooth. Therefore the standard rules of differential and integral calculus (as opposed to the ‘‘Itô calculus’’ [14]) apply when evaluating the integral in Eq. (5) and similar integrals below.

In regime I, one may approximate $f[x(t_1), t_1] \approx f[x(t), t_1]$, as pointed out above. In this regime, the fluctuations of f at a given point x are indistinguishable from the fluctuations of f along a particle trajectory. In this case, it is straightforward to determine the fluctuations of δx : since the force is assumed to have vanishing mean, Eq. (3), one has $\langle \delta x \rangle = 0$. The variance of δx is determined by making use of the fact that $\langle f(t)f(0) \rangle$ is small unless $|t| < \tau$. Evaluating $\langle \delta x^2 \rangle$, one finds the standard result

$$\langle \delta x^2 \rangle = \frac{2D_0 \delta t}{(m\gamma)^2}, \quad (6)$$

where D_0 is given by

$$D_0 = \frac{1}{2} \int_{-\infty}^{\infty} dt \langle f(t)f(0) \rangle. \quad (7)$$

The position $x(t)$ at time $t = N\delta t$ of a particle after N microscopic steps is $x(t) - x(0) = \sum_{i=1}^N \delta x_i$, where δx_i is the increment at the time step number i . For the diffusion constant, one obtains in the usual fashion

$$\mathcal{D}_x = \lim_{t \rightarrow \infty} \frac{\langle [x(t) - x(0)]^2 \rangle}{2t} = \lim_{t \rightarrow \infty} \sum_{i,j=1}^N \frac{\langle \delta x_i \delta x_j \rangle}{2\delta t N} = \frac{D_0}{(m\gamma)^2}, \quad (8)$$

where the increments δx_i and δx_j are statistically independent when $i \neq j$ and $\delta t \gg \tau$.

Consider now the underdamped regimes Ib and Ic. The displacements δp of momentum (for a short-time interval δt) obey

$$\delta p = -\gamma p \delta t + \delta w, \quad (9)$$

with

$$\delta w = \int_t^{t+\delta t} dt_1 f[x(t_1), t_1]. \quad (10)$$

In regimes Ib and Ic, the force fluctuates sufficiently rapidly compared to the time scale on which the momentum relaxes ($\omega \ll 1$) and the change δp of momentum during one correlation time of the force is small compared to the typical value of p . Consequently, Eq. (9) is a Langevin equation [7], describing the standard Ornstein-Uhlenbeck process where δw is Gaussian distributed with

$$\langle \delta w \rangle = 0, \quad \langle \delta w^2 \rangle = 2D_0 \delta t. \quad (11)$$

From the corresponding Fokker-Planck equation for the distribution $P(p, t)$ of momentum p at time t [7]

$$\frac{\partial P}{\partial t} = \frac{\partial}{\partial p} \left(\gamma p + D_0 \frac{\partial}{\partial p} \right) P, \quad (12)$$

one deduces that the steady-state distribution of momentum is Gaussian, $P(p) \propto \exp(-\gamma p^2 / 2D_0)$.

Also in this underdamped regime, the particles diffuse. The Fokker-Planck equation (12) allows to determine the correlation function of momentum in the steady state. The result is [7]

$$\langle p(t_1)p(t_2) \rangle_{\text{steady state}} = \frac{D_0}{\gamma} \exp(-\gamma |t_2 - t_1|). \quad (13)$$

This result in turn allows to calculate the diffusion constant

$$\begin{aligned} \mathcal{D}_x &= \lim_{t \rightarrow \infty} \frac{\langle x(t)^2 \rangle}{2t} \\ &= \lim_{t \rightarrow \infty} \frac{1}{2tm^2} \int_0^t dt_1 \int_0^t dt_2 \langle p(t_1)p(t_2) \rangle_{\text{steady state}} \\ &= \frac{D_0}{(m\gamma)^2}. \end{aligned} \quad (14)$$

By comparing Eqs. (8) and (14) one finds that the diffusion constant is the same in the over- and the underdamped limits,

$$\mathcal{D}_x = \frac{D_0}{(m\gamma)^2} \propto \frac{\xi^2}{\tau} \frac{\chi^2}{\omega^2}. \quad (15)$$

Figure 2 shows results of numerical simulations for the diffusion constant of the model defined by Eqs. (2)–(4). In the Ornstein-Uhlenbeck regime (I) the simulations agree well with Eq. (15).

We now briefly summarize what is known about the path-coalescence transition which distinguishes regime Ib from Ic. In the path-coalescing phase (regime Ib), particle trajectories governed by the equation of motion (2) coalesce, whereas in regime Ic, initially close particle trajectories separate almost surely (see Fig. 4). As was argued in [4], the maximal Lyapunov exponent λ serves as an ‘‘order parameter’’ for the phase transition. The exponent describes the rate of change of an infinitesimal separation between two trajectories

$$\lambda = \lim_{t \rightarrow \infty} t^{-1} \ln \left| \frac{\delta x_t}{\delta x_0} \right|. \quad (16)$$

Here, δx_0 is the initial separation of two infinitesimally close trajectories and δx_t is their separation at time t .

In regime Ib, the Lyapunov exponent is negative while it is positive in regime Ic. The condition for the phase transition is thus $\lambda = 0$. In regime I, the Lyapunov exponent can be calculated exactly [4]. Expressed in terms of the dimensionless parameters χ and ω , the phase transition is found to occur at

$$\omega \chi^{-2/3} = \text{const} \quad \text{as } \chi \rightarrow 0. \quad (17)$$

Figure 3 shows results of numerical simulations for the locus of the path-coalescence transition in the χ – ω plane for the model given by Eqs. (2)–(4). In regime I, the transition line is given by a line of slope 2/3, as expected from Eq. (17).

To conclude this section, we briefly discuss the asymptotic conditions delineating regime I in Fig. 1. First, in the overdamped limit, it was assumed that the distance covered in time τ is smaller than ξ . Estimating the advective velocity by $\sigma/(m\gamma)$, we have the condition $\sigma\tau/(m\gamma) \ll \xi$. Consequently, the condition distinguishing regimes Ia and IIb amounts to ω/χ approaching a constant when $\omega \rightarrow \infty$ and $\chi \rightarrow \infty$. Second, in the underdamped limit, $\omega \ll 1$, the boundary between regimes Ic and II is parametrized by the condition that ω/χ^2 approaches a constant when $\omega \rightarrow 0$ and $\chi \rightarrow 0$. This condition is derived in the next section [Eq. (33)], where regime II is discussed.

IV. GENERALIZED ORNSTEIN-UHLENBECK REGIME

We term the regime II in the phase diagram Fig. 1 the generalized Ornstein-Uhlenbeck regime. This regime is defined by strong stochastic forcing: the particles move fast and their momenta can be much larger than $p_0 = m\xi/\tau$. This means that the particle may travel many correlation lengths ξ during one correlation time τ and the stochastic force acting on the particle may decorrelate in a time which is small compared to τ . Thus the ‘‘effective correlation time’’ of the force $\xi m / \sqrt{\langle p^2 \rangle}$ can be much smaller than τ . It is also assumed that the dynamics of regime II is underdamped, i.e., $\omega \ll 1$.

A Fokker-Planck description is adequate in this regime. Define the increment δw of the force for a small time interval δt ,

$$\delta w = \int_t^{t+\delta t} dt_1 f[x(t_1), t_1]. \quad (18)$$

In regime I, the time dependence of $x(t_1)$ could be neglected, but this approximation is no longer valid when the forcing is strong. Instead, one integrates the equation of motion Eq. (2) to obtain $x(t) = x(0) + \delta x$, where

$$\delta x = \frac{1}{m} \int_0^{\delta t} dt_1 e^{-\gamma t_1} \left\{ p(0) + \int_0^{t_1} dt_2 e^{\gamma t_2} f[x(t_2), t_2] \right\}. \quad (19)$$

For times smaller than the small time interval δt , δx is small and one may expand the force around $\delta x = 0$. To lowest order in δt , one obtains

$$\begin{aligned} \langle \delta w \rangle &\approx \int_0^{\delta t} dt_1 \left\langle \frac{\partial f}{\partial x} [x(0), t_1] \delta x \right\rangle \\ &\approx \frac{1}{m} \int_0^{\delta t} dt_1 \int_0^{t_1} dt' \int_0^{t'} dt'' e^{-\gamma(t'-t'')} \\ &\quad \times \left\langle \frac{\partial f}{\partial x} [x(0), t_1] f[x(t''), t''] \right\rangle, \end{aligned} \quad (20)$$

where we have used that $\langle f[x(0), t] \rangle = 0$. Since it is assumed that $\omega = \gamma\tau \ll 1$, the exponent $\gamma(t' - t'') \approx 0$ and the major contribution to the integrals from the force correlation is for $|t_1 - t''| < \tau$. We obtain

$$\langle \delta w \rangle \approx \frac{\delta t}{2m} \int_{-\infty}^{\infty} dt t \left\langle \frac{\partial f}{\partial x} (0, 0) f(pt/m, t) \right\rangle. \quad (21)$$

The variance of the force increments (18) becomes to lowest order in δt ,

$$\begin{aligned} \langle \delta w^2 \rangle &= \int_0^{\delta t} dt_1 \int_0^{\delta t} dt_2 \langle f(pt_1/m, t_1) f(pt_2/m, t_2) \rangle \\ &\approx \delta t \int_{-\infty}^{\infty} dt C(pt/m, t), \end{aligned} \quad (22)$$

where C is the correlation function of the force (3).

Using that the change δp of momentum during a short-time period is $\delta p = -\gamma p \delta t + \delta w$ together with the first two moments of δw [Eqs. (21) and (22)], a Fokker-Planck equation is obtained using the standard procedure [7]

$$\frac{\partial P}{\partial t} = \frac{\partial}{\partial p} \left(-v(p) + \frac{\partial}{\partial p} D(p) \right) P. \quad (23)$$

Here, the drift and diffusion coefficients are

$$\begin{aligned} v(p) &= \lim_{\delta t \rightarrow 0} \frac{\langle \delta p \rangle}{\delta t} = -\gamma p + \frac{\partial}{\partial p} D(p), \\ D(p) &= \lim_{\delta t \rightarrow 0} \frac{\langle \delta p^2 \rangle}{2\delta t} = \frac{1}{2} \int_{-\infty}^{\infty} dt C(pt/m, t), \end{aligned} \quad (24)$$

where it was used that $\langle \delta w \rangle = \delta t \partial_p D(p)$. The above expression for the momentum diffusion coefficient $D(p)$ was earlier obtained in [9] and has also been used in [10] and [11]. Note that when $|p| \ll p_0$, $D(p) \approx D_0$, which corresponds to the Fokker-Planck equation of the standard Ornstein-Uhlenbeck process discussed in Sec. III.

On the other hand, when $|p| \gg p_0$, we approximate

$$D(p) = \frac{D_1 p_0}{|p|} + O(p^{-2}), \quad D_1 = \frac{m}{2p_0} \int_{-\infty}^{\infty} dX C(X, 0). \quad (25)$$

For the correlation function Eq. (4), we obtain $D(p) = D_0 / (1 + p^2/p_0^2)^{1/2}$, that is $D_1 = D_0$.

If the force is the gradient of a potential $V(x, t)$ with continuous derivatives, D_1 vanishes and $D(p) \propto |p|^{-3}$ provided $V(x, t)$ is sufficiently differentiable. Further, if the correlation function exhibits a cusp at $t=0$ (an example is discussed in [13]), we find $D(p) \propto |p|^{-2}$. In general, we write

$$D(p) = D_\zeta \left(\frac{p_0}{|p|} \right)^\zeta, \quad (26)$$

with $\zeta \geq 0$. In this paper, we mainly discuss the case $\zeta = 1$ which is a generic case for a random force [realized by the correlation function given in Eq. (4)]. But in Sec. VI, we briefly mention what is known for other force models giving rise to $\zeta \neq 1$.

The steady-state solution $P(p)$ of Eq. (23) is given by

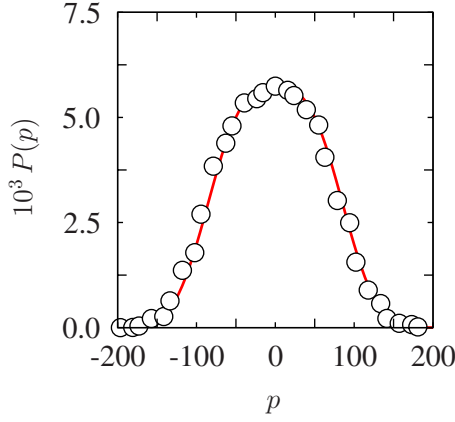


FIG. 5. (Color online) Non-Gaussian distribution of momentum in regime II (cf. Fig. 1). Shown are results of numerical simulations of Eq. (2) for $\chi=50$ and $\omega=0.01$ (circles) compared to Eq. (28) (red line).

$$P(p) = C \exp\left(-\gamma \int_0^p dp' \frac{p'}{D(p')}\right). \quad (27)$$

where C is chosen to normalize the distribution. When $D(p) \approx D_0$, the function $P(p)$ is approximately Gaussian, which corresponds to the standard Ornstein-Uhlenbeck regime (regimes Ib and Ic). When $D(p) = D_1 p_0 / |p|$, however, the distribution $P(p)$ is non-Gaussian (regime II) [12]

$$P(p) \sim \exp\left(-\frac{\gamma |p|^3}{3p_0 D_1}\right). \quad (28)$$

This result is compared to results of numerical simulations of Eqs. (2)–(4) in Fig. 5.

The generalized Ornstein-Uhlenbeck regime was studied in Ref. [12] (see also Ref. [13]). The Fokker-Planck equation (23) was solved as an eigenvalue problem and the propagator to reach momentum p at time t given the initial momentum was found. From this propagator, the momentum correlation function at equilibrium was calculated

$$\begin{aligned} \langle p(t') p(t'') \rangle_{\text{steady state}} &= \frac{\Gamma(4/3)}{3^{1/3} \Gamma(5/3)} \left(\frac{p_0 D_1}{\gamma} \right)^{2/3} e^{-2\gamma |t' - t''|} F_{21} \left(\frac{1}{3}, \frac{1}{3}; \frac{5}{3}; e^{-3\gamma |t' - t''|} \right), \end{aligned} \quad (29)$$

where F_{21} is a hypergeometric function [15].

From the momentum correlation function, Eq. (29), it is possible to calculate the diffusion constant in regime II. The result is [12]

$$D_x = \frac{(p_0 D_1)^{2/3}}{m^2 \gamma^{5/3}} \frac{\pi 3^{-5/6}}{2\Gamma(2/3)^2} F_{32} \left(\frac{1}{3}, \frac{1}{3}, \frac{2}{3}; \frac{5}{3}, \frac{5}{3}; 1 \right), \quad (30)$$

where F_{32} is a hypergeometric function. Since $D_1 \sim \sigma^2 \tau$, the diffusion constant D_x scales as

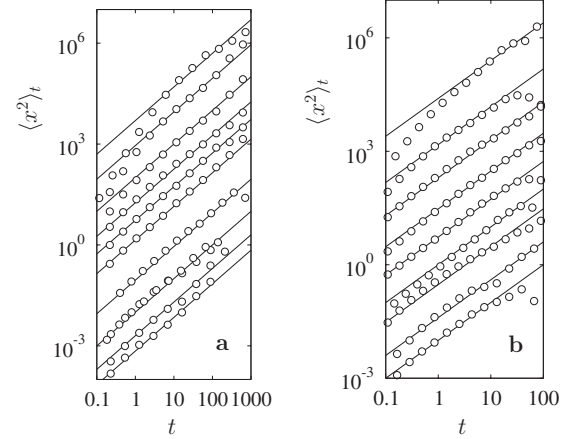


FIG. 6. Shows $\langle x^2 \rangle_t$ as a function of t ; (a) $\chi=50$ and $\omega=0.025, 0.075, 0.25, 0.5, 1, 2.5, 50, 200, 500$, and 800 , from top to bottom; (b) $\chi=1250$ and $\omega=0.125, 1, 0.5, 2.5, 5, 50, 100, 250, 1250, 2500$, and 5000 , from top to bottom. Solid lines are fits (as judged by the eyes) to the diffusion law (1). The corresponding values of D_x are shown in Fig. 2.

$$D_x \sim \frac{\xi^2}{\tau} \chi^{4/3} \omega^{-5/3}. \quad (31)$$

This result should be contrasted with Eq. (15). Figure 2 shows results of numerical simulations of the diffusion constant for our model [Eqs. (2)–(4)] in this regime, in good agreement with Eq. (30). The diffusion constant D_x was numerically determined by estimating $\langle x^2(t) \rangle / (2t)$, according to Eq. (1). Corresponding data are shown in Fig. 6. The dynamics in the generalized Ornstein-Uhlenbeck regime exhibits anomalous diffusion at short times [12,13]. Results of numerical experiments exhibiting anomalous diffusion are given in [12].

To conclude this section, we discuss the conditions under which the results described above are applicable. First, we discuss the asymptotic conditions in Fig. 1 defining the limits of regime II. The discussion above assumes that the dynamics in regime II are described by a Fokker-Planck equation (23) and we must also consider the conditions under which this equation is applicable.

Regime II is defined by the condition that the motion is underdamped, $\omega \ll 1$, and by the condition that the correlation time along the particle trajectory is smaller than the correlation time for a static particle. The latter condition defines the transition between regimes I and II in the phase diagram Fig. 1. This transition occurs when $\gamma p_0^2 / D_0$ is of order unity. This fact is most easily seen by determining the steady-state distribution $P(p)$ of momentum for the particular form, Eq. (4), of the correlation function $P(p) = C \exp(-\frac{\gamma p_0^2}{3D_0} [(1+p^2/p_0^2)^{3/2} - 1])$. In terms of the dimensionless parameters ω and χ , the above condition becomes

$$\frac{\gamma p_0^2}{D_0} \sim \frac{\gamma m^2 \xi^2}{\sigma^2 \tau^3} = \frac{\omega}{\chi^2} = \text{const.} \quad (32)$$

Thus the lines distinguishing the boundaries of regime II in the phase diagram in Fig. 1 are

$$\begin{aligned} \omega &= \text{const} \quad \text{as } \chi \rightarrow 0, \\ \omega/\chi^2 &= \text{const} \quad \text{as } \omega, \chi \rightarrow 0 \end{aligned} \quad (33)$$

Consider finally the conditions of validity of the Fokker-Planck equation (23) in regime II. For a Fokker-Planck description of a stochastic process to be valid, two necessary conditions must hold

(i) *Amplitude condition.* The random jumps of the stochastic variable must be much smaller than its typical size. Therefore, we must require that the change of momentum Δp during a correlation time of the forcing is much smaller than $\sqrt{\langle p^2 \rangle}$. This condition can be written in the form

$$\frac{\Delta p}{p} \sim \frac{\sigma m \xi}{p} \sim \frac{\sigma m \xi}{\langle p^2 \rangle} \sim \chi \left(\frac{\omega}{\chi^2} \right)^{2/3} \ll 1. \quad (34)$$

Here, we used the fact that the correlation time of the force is of the order of $m\xi/\sqrt{\langle p^2 \rangle}$ and that in the steady state $\sqrt{\langle p^2 \rangle} \sim (p_0 D_1 / \gamma)^{1/3} \sim p_0 (\chi^2 / \omega)^{1/3}$. The amplitude condition is thus fulfilled provided $\omega^2 / \chi \ll 1$.

(ii) *Frequency condition.* The stochastic forcing must fluctuate more rapidly than the stochastic variable. The correlation time of the force is of the order of $m\xi/\sqrt{\langle p^2 \rangle}$ and the relaxation time of p is of the order of γ^{-1} . We must therefore require that

$$\frac{\gamma \xi m}{\sqrt{\langle p^2 \rangle}} \sim \omega \left(\frac{\omega}{\chi^2} \right)^{1/3} \ll 1. \quad (35)$$

The frequency condition thus amounts to the same condition as above.

In our model, the amplitude and frequency conditions may not be sufficient to ensure that Eq. (23) is valid. The reason is that the fluctuations experienced by the particle may be influenced by the random force altering the trajectory of the particle, so that the trajectory does not explore the random force field ergodically. In addition to the two conditions above, the following self-consistency condition must also be satisfied:

(iii) *Self-consistency condition.* It is required that in the steady state, the particle moves sufficiently rapidly so that it is not captured by “valleys” in the potential corresponding to $f(x, t)$,

$$\langle p^2 \rangle / (2m) \gg \xi \sigma. \quad (36)$$

This condition too corresponds to $\omega^2 / \chi \ll 1$.

Within the boundaries of region II, we have $\omega \ll 1$ and $\omega / \chi^2 \ll 1$. In this limit, the condition $\omega^2 / \chi \ll 1$ is always satisfied, so that the Fokker-Planck equation is in fact always applicable in regime II for the type of random force model with $\zeta = 1$. In Sec. VI, we shall see that this may not be true for other values of ζ .

V. MINIMUM-TRACKING REGIME

We term the regimes III in the phase diagram Fig. 1 the “minimum-tracking regimes.” These regimes are defined by large damping $\omega \gg 1$ and strong stochastic forcing $\chi / \omega \gg 1$. When the force becomes large enough, the particle may be

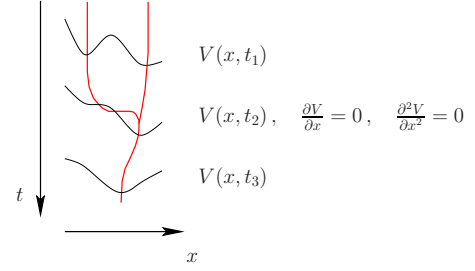


FIG. 7. (Color online) Disappearance of a minimum in $V(x, t)$ (thin black lines) and corresponding coalescence of particle trajectories (thick red lines) schematic.

come stuck in minima of the potential $V(x, t) = -\int_0^x dx' f(x', t)$ of the force.

The minimum-tracking regimes are divided into two distinct dynamical regimes: under- and overdamped minimum trackings. In the underdamped regime IIIa, the particle can oscillate around the potential minimum, whereas in the overdamped regime IIIb, such oscillations are quickly damped out (Fig. 2).

In regime IIIb, the diffusion constant is estimated as follows. Typically the particles are stuck in minima. As these minima randomly disappear and appear, the particle trajectories jump and may coalesce (Fig. 7). We argue that the diffusion constant is given in terms of the typical size of the valleys (ξ) and the rate at which they disappear. This rate can be estimated using a generalization of the method discussed in [16,17] for counting the zeroes of a random function $F(\mathbf{y})$. According to [16], the density ϱ of zeroes of the random function $F(\mathbf{y})$ is given by

$$\varrho = \langle \delta(F) | \det \mathbf{G} \rangle, \quad (37)$$

with $G_{\alpha\beta} = \partial F_{\alpha} / \partial y_{\beta}$.

Valleys disappear at inflection points of $V(x, t)$ and we thus need to count the joint zeroes of f and $\partial_x f \equiv f'$,

$$\varrho = \langle \delta(f) \delta(f') | \det \mathbf{G} \rangle, \quad (38)$$

with

$$\mathbf{G} = \begin{pmatrix} f' & \frac{\partial f}{\partial t} \\ f'' & \frac{\partial f'}{\partial t} \end{pmatrix}. \quad (39)$$

We need to calculate the average with respect to the set of Gaussian random variables $a_i = \{f, f', f'', \partial_t f, \partial_t f'\}$. The expectations of all five random variables vanish and their covariances Σ_{ij} can be expressed in terms of derivatives of the correlation function $C(x, t)$. For the special case (4), we obtain the covariance matrix

(ii) *Frequency condition.* In the steady state, we require

$$\gamma\xi m/\sqrt{\langle p^2 \rangle} \sim \omega \left(\frac{\omega}{\chi^2} \right)^{1/(2\zeta+1)} \ll 1. \quad (50)$$

(iii) *Self-consistency condition.* For general values of ζ , the self-consistency condition (36) yields

$$\frac{2m\xi\sigma}{\langle p^2 \rangle} \sim \chi \left(\frac{\omega}{\chi^2} \right)^{2/(2\zeta+1)} \ll 1. \quad (51)$$

This is the same condition as Eq. (49).

For $\zeta=1$, these three conditions are equivalent and correspond to the condition $\omega^2/\chi \ll 1$ derived in Sec. IV. But for other values of ζ , the conditions are no longer equivalent. Condition (51) can be written as

$$\omega \ll \chi^{3/2-\zeta}. \quad (52)$$

This result corresponds to a line with slope $-(\zeta-\frac{3}{2})^{-1}$ in Fig. 1. For $\zeta < 3/2$, this condition is satisfied everywhere in region II and therefore does not pose an additional constraint on the validity of the Fokker-Planck equation (23).

For $\zeta > 3/2$, by contrast, Eq. (52) is not satisfied everywhere in regime II. A new nonergodic region thus appears in the phase diagram above the dividing line determined by the condition $\omega\chi^{-3/2+\zeta} = \text{const}$ as $\chi \rightarrow \infty$. In this new regime, the theory put forward in [12,13] is inappropriate because the conditions for applying the Fokker-Planck approximation are not met. We have not been able to derive a theory describing the diffusion in this regime.

VII. CONCLUSIONS

In this paper, we studied the dynamics of particles subjected to random forcing and a damping mechanism which prevents the particles from being accelerated to arbitrarily high velocities. We considered the simplest model for such a process, Eqs. (1) and (2), which is a natural extension of the standard Ornstein-Uhlenbeck process.

It is expected that the particles undergo diffusion and our results support this expectation. More surprisingly, we show that the model exhibits a large number of diffusive regimes differing in the way in which the diffusion is microscopically realized. These regimes are summarized in Fig. 1 which is the main result of our paper. This asymptotic phase diagram is parametrized by dimensionless measures of the forcing, ω , and of the damping, ω .

The lines in Fig. 1 represent boundaries between the different dynamical regimes in the limits of large or small values of the dimensionless parameters. In the regimes Ia, Ib,

and Ic, the diffusion constant is given by the standard Ornstein-Uhlenbeck result [Eq. (15)].

In regime II, the diffusion constant scales with ω and χ in a manner different from the Ornstein-Uhlenbeck form, as first pointed out in [12,13]. For a generic random potential, the diffusion constant is given by Eq. (31). We remark that at short times, the particle positions and momenta exhibit anomalous diffusion [10–13]. It must be noted that there are particular choices of correlation function [Eq. (2)] for which region II is divided into two parts: one where the theory put forward in [12,13] applies and one where it fails, as shown in Sec. VI of this paper.

In regime III, finally, particles track the dynamics of the minima of the potential. This regime had not been analyzed before, we find that the diffusion constant is independent of ω and ξ [Eq. (42)]. The asymptotic scaling laws Eqs. (15), (31), and (42) agree reasonably well with results of numerical simulations (Fig. 2).

The model studied in this paper is known to exhibit a path-coalescence transition [4]. In the limit of $\omega \rightarrow 0$ and $\chi \rightarrow 0$, the locus of the phase transition is exactly known [4]. In this paper, we have numerically determined the phase-transition line in the ω - χ plane (Fig. 3). For small values of χ , the locus of the phase transition scales with the dimensionless parameters in a universal fashion [Eq. (17)] independently of the choice of correlation function [Eq. (2)]. At large values of χ , by contrast, our results show that the phase-transition line depends upon the correlation function and we have not been able to produce a theory predicting the locus of the phase transition. It is remarkable that the phase diagram of the fundamental one-dimensional model for diffusion processes studied here has not been completely characterized before now.

The results summarized above raise the question: what is known in higher dimensions? A theory for the path-coalescence transition in two and three dimensions in the limit of small values of χ was put forward in [19,20]. Less is known about the diffusion in two or three spatial dimensions in the generalized Ornstein-Uhlenbeck and the minimum-tracking regimes. In the generalized Ornstein-Uhlenbeck regime, it is possible to compute the steady-state momentum distribution in two and three spatial dimensions and to exactly characterize the short-time anomalous diffusion. These topics will be addressed in a forthcoming paper.

ACKNOWLEDGMENTS

This work was supported by Vetenskapsrådet (B.M.) and by the platform “Nanoparticles in an interactive environment” at Göteborg University (K.G. and B.M.).

[1] M. R. Maxey, *J. Fluid Mech.* **174**, 441 (1987).
 [2] M. Wilkinson, B. Mehlig, S. Östlund, and K. P. Duncan, *Phys. Fluids* **19**, 113303 (2007).
 [3] J. Deutsch, *J. Phys. A* **18**, 1449 (1985).
 [4] M. Wilkinson and B. Mehlig, *Phys. Rev. E* **68**, 040101(R),

(2003).
 [5] G. Falkovich, K. Gawędzki, and M. Vergassola, *Rev. Mod. Phys.* **73**, 913 (2001).
 [6] G. E. Uhlenbeck and L. S. Ornstein, *Phys. Rev.* **36**, 823 (1930).

- [7] N. G. van Kampen, *Stochastic Processes in Physics and Chemistry*, 2nd ed. (North-Holland, Amsterdam, 1981).
- [8] E. Fermi, *Phys. Rev.* **75**, 1169 (1949).
- [9] P. A. Sturrock, *Phys. Rev.* **141**, 186 (1966).
- [10] L. Golubovic, S. Feng, and F.-A. Zeng, *Phys. Rev. Lett.* **67**, 2115 (1991).
- [11] M. N. Rosenbluth, *Phys. Rev. Lett.* **69**, 1831 (1992).
- [12] E. Arvedson, M. Wilkinson, B. Mehlig, and K. Nakamura, *Phys. Rev. Lett.* **96**, 030601 (2006).
- [13] V. Bezuglyy, B. Mehlig, M. Wilkinson, K. Nakamura, and E. Arvedson, *J. Math. Phys.* **47**, 073301 (2006).
- [14] C. W. Gardiner, *Handbook of Stochastic Methods: For Physics, Chemistry and the Natural Sciences*, 3rd ed. (Springer, Berlin, 2004).
- [15] M. Abramowitz and I. A. Stegun, *Handbook of Mathematical Functions*, 9th ed. (Dover, New York, 1972).
- [16] M. Kac, *Bull. Am. Math. Soc.* **49**, 314 (1943).
- [17] S. O. Rice, *Bell Syst. Tech. J.* **24**, 46 (1945).
- [18] G. Falkovich, S. Musacchio, L. Piterbarg, and M. Vucelja, *Phys. Rev. E* **76**, 026313 (2007).
- [19] B. Mehlig and M. Wilkinson, *Phys. Rev. Lett.* **92**, 250602 (2004).
- [20] B. Mehlig, M. Wilkinson, K. Duncan, T. Weber, and M. Ljunggren, *Phys. Rev. E* **72**, 051104 (2005).